

Size-dependent electronic eigenstates of multilayer organic quantum wells

Nguyen Ba An^{†§} and Eiichi Hanamura[‡]

[†] International Centre for Theoretical Physics, Trieste, Italy

[‡] Department of Applied Physics, University of Tokyo, 7-3-1 Hongo, Bunkyo-ku, Tokyo 113, Japan

Received 20 October 1995, in final form 17 January 1996

Abstract. A detailed theoretical treatment is given of eigenfunctions and eigenenergies of a multilayer organic quantum well sandwiched between two different dielectric media. The abrupt change of dielectric constants at the interfaces distorts the wave function and results in there being possible surface states in addition to propagating states. The proper boundary conditions are accounted for by the method of image charges. Analytic criteria for the existence of surface states are established using the nearest-layer approximation; they depend not only on the intralayer and interlayer parameters but also on the number of layers. The size dependence together with the dependence on signs and relative magnitudes of the structure parameters fully determine the energy spectrum of propagating states as well as the number and the location of surface states.

1. Introduction

Manipulation technologies for semiconductors [1] and organic materials [2] have been developed and so quantization effects and dimensional effects of electronic excitations have been clarified. At the same time one can control (i) the radiation field via the microcavities and (ii) the manipulated semiconductor quantum wells via the distributed Bragg reflectors at both ends. Combining the results, efforts are being made to realize a strong interaction between quantized electronic excitations and quantized modes of the radiation field via mutual quantum control of the two systems on the same footing. The nonclassical nature of the radiation field can be established from investigation of these systems. Recently, unusual structures have been quasi-epitaxially grown for the first time by the novel technique of organic molecular beam deposition [3, 4]. These structures are called multiple organic quantum wells (MOQWs); they consist of alternating layers of two different organic materials. Thanks to the weakness of the van der Waals forces that hold the molecules together, organic heterostructures can even be grown alternatively in incommensurate materials like 3,4,9,10 perylenetetracarboxylic dianhydride and 3,4,7,8 naphthalenetetracarboxylic dianhydride [3]. Each molecule in organic materials has a large transition dipole moment in comparison to those of the unit cells of semiconductors, and the electronic transitions in organic materials are primarily due to the generation of Frenkel

[§] Now at: National Centre for Natural Sciences and Technology, Institute of Physics, PO Box 429, Bo Ho, Hanoi 10000, Vietnam.

excitons—which are coherent elementary excitations. So, (M)OQWs have proven to provide one of the most promising areas for studying molecular Frenkel and charge-transfer excitons as well as various potential device applications [5, 6, 7, 8]. Although the electronic structures and optical properties of semiconductor quantum wells have been well studied [1], some characteristics of (M)OQWs remain undiscovered as yet. In this paper we are concerned with the electronic structure of a multilayer OQW. The super-radiance property of OQWs has been investigated recently in [9]; however, the interaction between crystalline layers was neglected in the investigation. Super-radiant decay can be described in terms of the imaginary part of the second-order self-energy due to exciton–photon interaction, while its real part gives the dipole–dipole interaction. Usually the absolute value of the dipole–dipole interaction is much larger than the radiative decay rate [10]. Therefore, it is natural to obtain the electronic structure of the Coulomb excitons with the dipole–dipole interaction taken into account before discussing the dynamics of surface excitons. In general, especially in crystals having a small spacing between layers, the interlayer coupling plays a crucial role in determining the eigenstates of the whole material structure. With the interlayer interaction taken into account, the excitation can hop from layer to layer and the resulting electronic structure is that of the whole OQW rather than that of separate layers. In this respect, it would not be so accurate to describe radiative rates as those coming from the first monolayer, the second monolayer, etc. Even in crystals like tetracene, anthracene, etc, whose Coulomb exciton band widths in the direction perpendicular to the layer planes are small as compared to other energy characteristics [11], experimental measurements should, in principle, be explained on the basis of the energy spectrum of the OQW as a whole. The lowest photo-excited elementary excitations in solids can be described as excitons. Although excitons are of Wannier–Mott type in inorganics, their nature in organics has remained unclear to date [12]. In some organics like strongly π -bonded 3,4,9,10 perylenetetracarboxylic dianhydride [13], (charge-transfer) excitons seem to have large radii as compared to the intermolecular separation resembling the Wannier–Mott type. Sometimes, in the same kind of structure—say, in PbI-based compounds—excitons have alternatively been considered as either of Frenkel type [14] or of Wannier–Mott type [15]. Moreover, coexistence of the two types of exciton is also possible [16]. We are not convinced of the importance of this debate and, in our model, we assume the excitons to be of Frenkel type. Frenkel excitons propagate over the structure via dipolar interaction among the constituent molecules. We introduce a model of multilayer OQWs with the dielectric constant ε sandwiched between continuum media with dielectric constants ε_1 and ε_2 . Due to an abrupt change of dielectric constants at the interfaces separating the OQW region from the two surrounding materials, surface states may be possible in some cases in addition to propagating states. In this paper we will describe the electronic structure of the multilayer OQW, trying to answer the questions of: (i) under which conditions surface states are possible; (ii) how many surface states may appear; (iii) where the surface state energy levels are located; and (iv) how the number of surface states depends on the thickness of the OQW.

The present paper is organized as follows. In section 2 we construct a Hamiltonian of the OQW taking into account the boundary conditions due to the abrupt change of the dielectric constants at the two interfaces by the method of image charges. Here the dielectric constants outside the OQW play a role in inducing surface states. In section 3 we derive the difference equations of the problem within the nearest-layer approximation (NLA) which are to be solved for the propagating states in section 4 and for the surface states in section 5. In section 6 we discuss the results obtained as well as related optical responses and future problems.

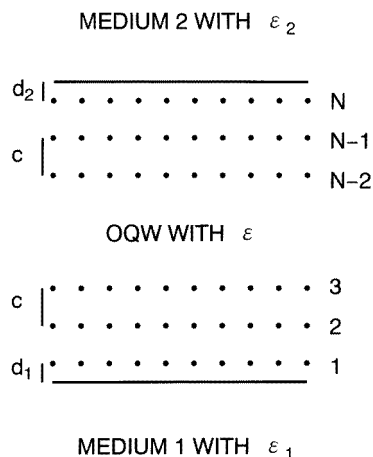


Figure 1. An N -layer OQW with dielectric constant ε sandwiched between two media with dielectric constants ε_1 and ε_2 . The interlayer separation is c . The effective distances from the outermost crystalline layers to the interfaces are d_1 and d_2 .

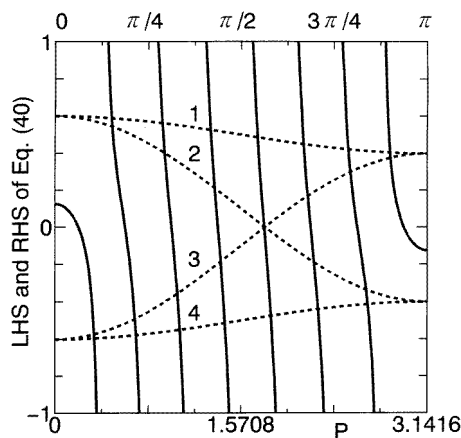


Figure 2. The LHS for $N = 8$ (solid lines) and RHSs (dashed curves) of equation (40) as functions of p taken from 0 to π . The dashed curves labelled 1, 2, 3 and 4 are those with $\zeta(\xi) = 0.5, 0.1, -0.1$ and -0.5 (0.1, 0.5, -0.5 and -0.1), respectively. The intersections of solid lines and dashed curves determine the allowed values of p and the number of them for the propagating states.

2. The multilayer organic quantum well and its Hamiltonian

Consider an N -layer OQW with dielectric constant ε . This OQW is sandwiched between two dielectric media with dielectric constants ε_1 and ε_2 (figure 1). Usually, medium 1 serves as an inorganic substrate ($\varepsilon_1 \neq \varepsilon$) and medium 2 is the open air ($\varepsilon_2 \approx 1$), or both of the surrounding media are of the same material ($\varepsilon_1 = \varepsilon_2 \neq \varepsilon$). In general, they are different, i.e., $\varepsilon_1 \neq \varepsilon_2 \neq \varepsilon$. The two interfaces are assumed to be smooth planes. Suppose that the unit cells of the OQW lattice contain identical two-level molecules—one in each cell—for simplicity (extensions to the case of more than one molecule per unit cell and to multilevel molecules can be made). At low excitation one molecule is excited. This excited molecule interacts with all other unexcited real molecules in the OQW regions as well as, due to the presence of the interfaces, with their images in the region of the surrounding materials (including the image of the excited molecule itself). Furthermore, the excitation can be transferred from cell to cell, which is also influenced by the image effect. The energy difference between the ground state of the OQW and the state in which one molecule is being excited is described by the Hamiltonian:

$$H = \sum_{lmn} (\epsilon - \epsilon_0 + A_n + \tilde{A}_n) P_{lmn}^+ P_{lmn} + \sum'_{lmn, l'm'n'} (T_{lmn, l'm'n'} + \tilde{T}_{lmn, l'm'n'}) P_{l'm'n'}^+ P_{lmn}. \quad (1)$$

In equation (1) l, m, n are integers specifying the position \mathbf{r} of the unit cell in terms of the basic vectors \mathbf{a}, \mathbf{b} and \mathbf{c} of the OQW:

$$\mathbf{r} = l\mathbf{a} + m\mathbf{b} + n\mathbf{c} \quad (2)$$

where $-N_a \leq l \leq N_a$, $-N_b \leq m \leq N_b$ and $n = 1, 2, \dots, N_c = N$. N_a (N_b) is the number of unit cells in the \mathbf{a} (\mathbf{b}) direction and N the number of layers perpendicular to the \mathbf{c} direction. The OQW is assumed to be substantially extended in the (\mathbf{a}, \mathbf{b}) plane (i.e.,

N_a and N_b are large in comparison with N and can be made infinite at the end of the calculations), but bounded in the c direction by two outermost layers (i.e., N is finite). As a consequence of such structure, the translational symmetry in the c direction is broken, whereas in the (a, b) plane the usual Born–von Karman cyclic condition can be used by treating N_a and N_b as finite but very large. The operator P_{lmn}^+ (P_{lmn}) converts the molecule in cell lmn from its ground state $|0\rangle$ (excited state $|x\rangle$) with energy ϵ_0 (ϵ) to its excited state $|x\rangle$ (ground state $|0\rangle$) with energy ϵ (ϵ_0). The term A_n (\tilde{A}_n) expresses the difference in energy caused by electrostatic interaction of the molecule in its excited state and unexcited state with all of the other unexcited real (image) molecules in the OQW. Due to the finite extent in the c direction, the n -dependence is retained in the terms A_n and \tilde{A}_n . These terms are the diagonal elements of H and are referred to as the site shift terms. The off-resonant elements of H , the terms $T_{lmn,l'm'n'}$ and $\tilde{T}_{lmn,l'm'\tilde{n}'}$, are responsible for intersite excitation transfer and are called the excitation transfer terms. Again the tilde signifies the image effect. The prime on the second sum in equation (1), which excludes the contribution from $l = l'$, $m = m'$ and $n = n'$ simultaneously, acts on T only, not on \tilde{T} . Actual expressions for A_n , \tilde{A}_n , $T_{lmn,l'm'n'}$ and $\tilde{T}_{lmn,l'm'\tilde{n}'}$ will be given later.

We split H into two parts, one for $n = n'$ and the other for $n \neq n'$:

$$H = \sum_n H_n + \sum_{nn'} H_{nn'}. \quad (3)$$

The part H_n

$$H_n = \sum_{lm} \left(\epsilon - \epsilon_0 + A_n + \tilde{A}_n \right) P_{lmn}^+ P_{lmn} + \sum'_{lm,l'm'} \left(T_{lmn,l'm'n} + \tilde{T}_{lmn,l'm'\tilde{n}} \right) P_{l'm'n}^+ P_{lmn} \quad (4)$$

can be exactly diagonalized by means of the unitary transformation

$$P_{lmn} = \frac{1}{\sqrt{N_a N_b}} \sum_{\mathbf{k}} B_{n\mathbf{k}} e^{i\mathbf{k} \cdot \boldsymbol{\rho}_{l,m}} \quad (5)$$

where $\boldsymbol{\rho}_{l,m} = l\mathbf{a} + m\mathbf{b}$, and \mathbf{k} is a two-dimensional wave vector of motion in the layers. The operator $B_{n\mathbf{k}}$ ($B_{n\mathbf{k}}^+$) is regarded as annihilating (creating) a two-dimensional exciton in layer n with energy $E_n(k)$:

$$E_n(k) = \epsilon - \epsilon_0 + A_n + \tilde{A}_n + L_n(k) \quad (6)$$

$$L_n(k) = \frac{1}{N_a N_b} \sum'_{lm,l'm'} \left(T_{lmn,l'm'n} + \tilde{T}_{lmn,l'm'\tilde{n}} \right) e^{i\mathbf{k} \cdot \boldsymbol{\rho}_{l-l',m-m'}}. \quad (7)$$

The two-dimensional sum in equation (7) can easily be evaluated, e.g. by a chainwise summation method [17]. Using equation (5) in the expression for $H_{nn'}$ we are able to convert equation (1) to a form that is entirely in terms of two-dimensional exciton operators:

$$H = \sum_{\mathbf{k}} \sum_n \left[E_n(k) B_{n\mathbf{k}}^+ B_{n\mathbf{k}} + \sum_{n' \neq n} R_{nn'}(k) B_{n'\mathbf{k}}^+ B_{n\mathbf{k}} \right] \quad (8)$$

with $R_{nn'}$ describing the interlayer coupling:

$$R_{nn'}(k) = \frac{1}{N_a N_b} \sum'_{lm,l'm'} \left(T_{lmn,l'm'n'} + \tilde{T}_{lmn,l'm'\tilde{n}'} \right) e^{i\mathbf{k} \cdot \boldsymbol{\rho}_{l-l',m-m'}}. \quad (9)$$

Evaluation of $R_{nn'}$ is also performable analytically for any n and $n' \neq n$. Studying a multilayer structure by first considering separate layers and then calculating interlayer interactions constitutes the so-called planewise method of summation [18]. Via such a method applied to dipolar interactions in organic networks, explicit dependences on the

lattice constants and orientations of transition dipole moments and wave vectors have recently been derived [17] showing quite interesting dimensional crossover effects as well as peculiarities concerning the optical responses.

A well recognized fact is that the interlayer interaction falls off very rapidly with increasing separation between layers [17, 18]. In many cases, the NLA suffices to explain experiments. We thus confine ourselves in this paper to the NLA only. The general expression for A_n is [19]

$$A_n \equiv A_{lmn} = \frac{1}{\varepsilon} \sum'_{l'm'n'} [\langle 0x | V_{lmn,l'm'n'} | 0x \rangle - \langle 00 | V_{lmn,l'm'n'} | 00 \rangle] \quad (10)$$

where $V_{lmn,l'm'n'}$ is the operator of the Coulomb interaction between molecules in cells lmn and $l'm'n'$, and $|0x\rangle$ denotes a state in which cell lmn is in the excited state and all others are in the ground state. In the NLA there are three distinct types of A_n : A_1 which couples layer 1 with layer 2, A_n ($1 < n < N$) which couples layer n with its two nearest layers $n \pm 1$, and A_N which couples layer N with layer $N - 1$. They are of the forms

$$A_1 = \frac{1}{\varepsilon} \sum_{l'm'} [\langle 0x | V_{lm1,l'm'2} | 0x \rangle - \langle 00 | V_{lm1,l'm'2} | 00 \rangle] \quad (11)$$

$$A_n = \frac{1}{\varepsilon} \sum_{l'm'} \sum_{n'=n\pm 1} [\langle 0x | V_{lmn,l'm'n'} | 0x \rangle - \langle 00 | V_{lmn,l'm'n'} | 00 \rangle] \quad (12)$$

$$A_N = \frac{1}{\varepsilon} \sum_{l'm'} [\langle 0x | V_{lmN,l'm'N-1} | 0x \rangle - \langle 00 | V_{lmN,l'm'N-1} | 00 \rangle]. \quad (13)$$

The general expression for the term \tilde{A}_n , is cumbersome because in the presence of two interfaces the number of image molecules is infinite even for a single real molecule. In principle, one can derive such an expression from first principles [20]. However, the NLA does not require this, which greatly simplifies the actual expressions to be used. In our model of multilayer OQWs, the dielectric constants ε_1 and ε_2 of the surrounding materials are well defined, but the interface distances d_1 and d_2 shown in figure 1 are treated as parameters of the order of or less than half an interlayer separation, $c/2$. Then, the image effect needs to be taken into account only for the two surface layers. For all of the internal layers with $1 < n < N$ we have $\tilde{A}_n = 0$, while

$$\tilde{A}_1 = \frac{\varepsilon - \varepsilon_1}{\varepsilon(\varepsilon + \varepsilon_1)} \sum_{l'm'} [\langle 0x | \tilde{V}_{lm1,l'm'\bar{1}} | 0x \rangle - \langle 00 | \tilde{V}_{lm1,l'm'\bar{1}} | 00 \rangle] \quad (14)$$

$$\tilde{A}_N = \frac{\varepsilon - \varepsilon_2}{\varepsilon(\varepsilon + \varepsilon_2)} \sum_{l'm'} [\langle 0x | \tilde{V}_{lmN,l'm'\bar{N}} | 0x \rangle - \langle 00 | \tilde{V}_{lmN,l'm'\bar{N}} | 00 \rangle]. \quad (15)$$

In equations (14) and (15), $\tilde{V}_{lm1,l'm'\bar{1}}$ ($\tilde{V}_{lmN,l'm'\bar{N}}$) is the operator of the Coulomb interaction between a real molecule in cell $lm1$ (lmN) and the image of a real molecule in cell $l'm'1$ ($l'm'N$), or, as we could equally say, the image molecule in image cell $l'm'\bar{1}$ ($l'm'\bar{N}$). The distance between layer 1 (N) and its image layer $\bar{1}$ (\bar{N}) equals $2d_1$ ($2d_2$). It is worth noting that the coordinates of the electrons and nuclei of a real molecule and its image are mirror symmetric. This feature should be treated with care when dealing with interactions due to dipoles or multipoles.

The general formula for $T_{lmn,l'm'n'}$ [19] is

$$T_{lmn,l'm'n'} = \frac{1}{\varepsilon} \langle 0x | V_{lmn,l'm'n'} | x0 \rangle \quad (16)$$

which is dominated by the dipole–dipole interactions [11]. For the term $\tilde{T}_{lmn,l'm'\tilde{n}'}$ only two contributions are of interest in the NLA; these are

$$\tilde{T}_{lm1,l'm'\tilde{1}} = \frac{\varepsilon - \varepsilon_1}{\varepsilon(\varepsilon + \varepsilon_1)} \langle 0x | \tilde{V}_{lm1,l'm'\tilde{1}} | x0 \rangle \quad (17)$$

$$\tilde{T}_{lmN,l'm'\tilde{N}} = \frac{\varepsilon - \varepsilon_2}{\varepsilon(\varepsilon + \varepsilon_2)} \langle 0x | \tilde{V}_{lmN,l'm'\tilde{N}} | x0 \rangle. \quad (18)$$

We therefore obtain in the NLA the following expressions for the L_n -terms of equation (7):

$$L_1(k) = L(k) + \frac{1}{N_a N_b} \sum_{lm,l'm'} \tilde{T}_{lm1,l'm'\tilde{1}} e^{ik \cdot \rho_{l-l',m-m'}} \quad (19)$$

$$L_n(k) = L(k) \quad 1 < n < N \quad (20)$$

$$L_N(k) = L(k) + \frac{1}{N_a N_b} \sum_{lm,l'm'} \tilde{T}_{lmN,l'm'\tilde{N}} e^{ik \cdot \rho_{l-l',m-m'}} \quad (21)$$

with

$$L(k) = \frac{1}{N_a N_b} \sum'_{lm,l'm'} T_{lmn,l'm'n} e^{ik \cdot \rho_{l-l',m-m'}} \quad (22)$$

which is independent of n in spite of the presence of n in its definition.

As for the interlayer interaction $R_{nn'}$ (k), in the NLA the image terms \tilde{T} in equation (9) do not contribute while the T -terms contribute only for $|n' - n| = 1$, i.e., for $n' = n \pm 1$. These two contributions (for $n' = n + 1$ and $n' = n - 1$) are equal to each other and can be denoted simply by $R(k)$:

$$R(k) = \frac{1}{N_a N_b} \sum_{lm,l'm'} T_{lmn,l'm'n \pm 1} e^{ik \cdot \rho_{l-l',m-m'}}. \quad (23)$$

We notice that in the NLA we have four parameters in all. The three intralayer parameters are $E_1(k)$, the energy of the first layer, $E_n(k) = E(k)$ for $1 < n < N$, the energy of the $N - 2$ internal layers, and $E_N(k)$, the energy of the N th layer. The only interlayer parameter is $R(k)$. Besides this, we also have N , the number of layers, as a parameter characterizing the thickness of the OQW. Determining the dependence of the eigenfunctions and eigenenergies of the OQW on $E_1(k)$, $E(k)$, $E_N(k)$, R and N is our aim in the following sections.

3. Difference equations

The eigenfunction of the OQW is represented as

$$\Psi_{\mathbf{k}} = \sum_{n=1}^N g_n(k) B_{n\mathbf{k}}^+ |0\rangle \quad (24)$$

where the expansion coefficients $g_n(k)$ are to be determined so as to satisfy the Schrödinger equation

$$H \Psi_{\mathbf{k}} = \omega_{\mathbf{k}} \Psi_{\mathbf{k}} \quad (25)$$

with $\omega_{\mathbf{k}}$ being the eigenenergy of the whole structure. When equations (8) and (24) are substituted into equation (25) we get the following equations for ω and g_n (the wave vector \mathbf{k} of the motion in the layer planes is omitted for brevity from now on):

$$(\omega - E_1)g_1 = Rg_2 \quad (26)$$

$$(\omega - E)g_n = R(g_{n-1} + g_{n+1}) \quad 1 < n < N \quad (27)$$

$$(\omega - E_N)g_N = Rg_{N-1}. \quad (28)$$

These are the difference equations that we need to solve. We first find the general solution to equation (27) and then require it to be a solution of the two special equations (26) and (28) too. It is easy to verify [21] that any of the four functions $\exp[(\pm\kappa \pm ip)nc]$, with κ and p real, obeys equation (27). The general solution of equation (27) is therefore a linear combination of these functions:

$$g_n = \alpha' x^n + \frac{\beta'}{x^n} + \theta' x^{*n} + \frac{\vartheta'}{x^{*n}} \quad (29)$$

where $x = \exp(\kappa + ip)c$ and α' , β' , θ' , ϑ' are as yet unknown coefficients, which may without loss of generality be assumed real. Putting equation (29) into equation (27) yields

$$\omega = E + 2RF \quad (30)$$

with

$$F = \frac{[\alpha' x^n + \beta'/x^n] \cosh(\kappa + ip)c + [\theta' x^{*n} + \vartheta'/x^{*n}] \cosh(\kappa - ip)c}{\alpha' x^n + \beta'/x^n + \theta' x^{*n} + \vartheta'/x^{*n}}. \quad (31)$$

Since ω is the eigenenergy of the whole multilayer structure, in which the layers are coupled, it should not depend on the layer index n explicitly. From equations (30) and (31), this is so provided that $\cosh(\kappa + ip)c = \cosh(\kappa - ip)c$ which leads to

$$\sinh(\kappa c) \sin(pc) = 0. \quad (32)$$

Either $\sinh(\kappa c)$ or $\sin(pc)$ must vanish, resulting in two possibilities only:

- case (i): $\kappa = 0$, $p \neq 0$; and
- case (ii): $\kappa \neq 0$, $pc = \pi j$, where j is an integer or zero.

It is easy to check that in case (i), g_n turns out to be determined by two (not four) coefficients only, namely

$$g_n = \alpha \cos(pcn) + \beta \sin(pcn). \quad (33)$$

Then $F = \cos(pc)$ and the eigenenergy ω is given by

$$\omega = E + 2R \cos(pc). \quad (34)$$

In case (ii), instead of equation (29), g_n reduces to

$$g_n = (-1)^{nj} [\theta e^{\kappa cn} + \vartheta e^{-\kappa cn}]. \quad (35)$$

Correspondingly, we have $F = (-1)^j \cosh(\kappa c)$ and

$$\omega = E + 2(-1)^j R \cosh(\kappa c). \quad (36)$$

We are left to determine α , β , p and θ , ϑ , κ , j such that equation (33) and equation (35) will also be solutions to the two special equations (26) and (28) as well as meeting the corresponding normalization condition required for the wave function, equation (24). The states which originate from case (i) resemble a wave propagating back and forth along the c direction due to the cosines and sines and—hence—are called propagating states. On the other hand, the states which originate from case (ii) represent an evanescent wave near the interfaces due to the exponential and—hence—are referred to as surface states. Apart from the different behaviours of the spatial profiles, equations (34) and (36) also reveal that on the energy scale the propagating states lie inside the interval $[E - 2|R|, E + 2|R|]$ —called the bulk band or simply the band—whereas the surface states are located outside that band. In what follows we shall clarify the question of how many surface states are possible and, if a surface state does exist, whether its energy level is located above or below the band.

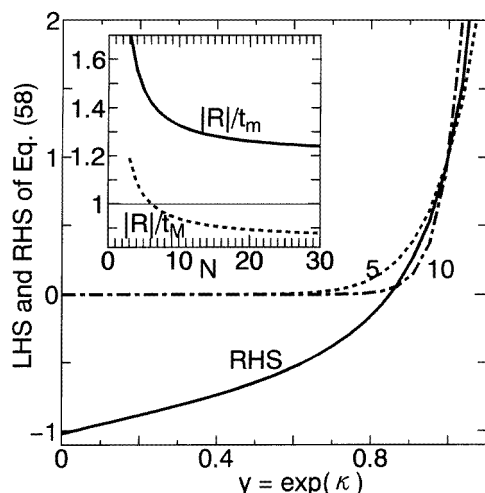


Figure 3. LHSs with $N = 5$ (dashed, labelled 5), $N = 10$ (chain, labelled 10) and the RHS (solid) of equation (58) for $\Delta_m \Delta_M < 0$, $|R/\Delta_m| = 1.2$ and $|R/\Delta_M| = 0.85$. One nontrivial intersection occurs for $N = 10$, while none are found for $N = 5$. The inset plots $|R|/t_m$ (solid) and $|R|/t_M$ (dashed) versus N . In this case N^* is determined by the intersection of $|R|/t_M$ and the straight line going through 1.

4. Propagating states

The notation is simplified by defining new parameters Δ_1 and Δ_N :

$$\Delta_1 = E - E_1 \quad \Delta_N = E - E_N \quad (37)$$

and by treating p and κ in units of the interlayer separation c . Using equation (33) we show that equation (26) is obeyed if

$$\alpha(\Delta_1 \cos p + R) + \beta \Delta_1 \sin p = 0 \quad (38)$$

whereas equation (28) demands

$$\tan(Np) - \frac{\alpha(\Delta_N + R \cos p) + \beta R \sin p}{\alpha R \sin p - \beta(\Delta_N + R \cos p)} = 0. \quad (39)$$

Eliminating α and β from equations (38) and (39) we arrive at an equation which determines the allowed values of p :

$$\sin p \cot Np = \zeta + \xi \cos p \quad (40)$$

with ζ and ξ given by

$$\zeta = \frac{R(\Delta_1 + \Delta_N)}{\Delta_1 \Delta_N - R^2} \quad \xi = \frac{\Delta_1 \Delta_N + R^2}{\Delta_1 \Delta_N - R^2}. \quad (41)$$

A plot of the LHS and RHS of equation (40) as functions of p for $N = 8$ is depicted in figure 2. The intersections of the two sides determine the allowed values of p and their number. Note that the propagating states here come from the exciton propagation in the direction perpendicular to the layer planes. The exciton propagation in the layers has already been accounted for above via the k -dependence of $\Delta_1(k)$, $\Delta_N(k)$ and $R(k)$. Sometimes, to make this feature explicit, k is denoted as k_{\parallel} and p as k_{\perp} .

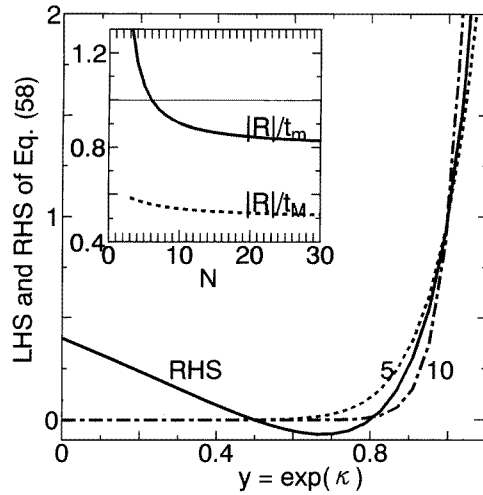


Figure 4. As figure 3, but for $\Delta_m \Delta_M > 0$, $|R/\Delta_m| = 0.8$ and $|R/\Delta_M| = 0.5$. Two nontrivial intersections occur for $N = 10$, while only one is found for $N = 5$. In this case N^* is determined by the intersection of $|R/t_m$ and the straight line going through 1.

Table 1. A summary of the dependence of the allowed number of propagating states on the signs of the functions f_+ and f_- defined by equation (42).

Row	sign(f_+)	sign(f_-)	Number of propagating states
1	+	0 or +	$N - 1$
2	+	-	$N - 2$
3	- or 0	0 or +	N
4	- or 0	-	$N - 1$

Now, it is not difficult to verify that the number of propagating states, i.e., the number of allowed values of p , is determined by the signs of two N -dependent quantities f_+ and f_- , defined as

$$f_{\pm} = \zeta \pm \xi \mp \frac{1}{N}. \quad (42)$$

Table 1 summarizes all of the possible situations (compare with figure 2). As the total number of states should be N , the situations corresponding to rows 1, 2 and 4 in table 1 reveal 'missing' states. As can be expected, these missing states are the surface states which originate from case (ii). To better understand the physics of the criteria determining the possible number of propagating states, we would rather 'translate' table 1 into the original physical parameters Δ_1 , Δ_N , R and N than read it in terms of f_+ and f_- . For that purpose, we rewrite f_+ and f_- as follows:

$$f_{\pm} = \frac{\pm(N+1)(R \mp t_1)(R \mp t_2)}{N(\Delta_1 \Delta_N - R^2)} \quad (43)$$

where

$$t_1 = \frac{-N(\Delta_1 + \Delta_N) - \sqrt{\delta}}{2(N+1)} \quad (44)$$

$$t_2 = \frac{-N(\Delta_1 + \Delta_N) + \sqrt{\delta}}{2(N+1)} \quad (45)$$

$$\delta = (N^2 - 1)(\Delta_1 - \Delta_N)^2 + (\Delta_1 + \Delta_N)^2. \quad (46)$$

We have performed a careful sign analysis of f_{\pm} with respect to N , and to signs and absolute values of Δ_1 , Δ_N and R . As a result, we have obtained the following criteria:

$$\begin{cases} t_M \leq |R|: & N \text{ propagating states} \\ t_m \leq |R| < t_M: & N - 1 \text{ propagating states} \\ |R| < t_m: & N - 2 \text{ propagating states.} \end{cases} \quad (47)$$

In the above criteria

$$t_m = \frac{|N|\Delta_1 + \Delta_N| - \sqrt{\delta}}{2(N+1)} \quad (48)$$

$$t_M = \frac{N|\Delta_1 + \Delta_N| + \sqrt{\delta}}{2(N+1)}. \quad (49)$$

At this point, several interesting remarks are worth making. When starting to deal with the problem, intuition might lead to the following criteria:

$$\begin{cases} |\Delta_M| \leq |R|: & N \text{ propagating states} \\ |\Delta_m| \leq |R| < |\Delta_M|: & N - 1 \text{ propagating states} \\ |R| < |\Delta_m|: & N - 2 \text{ propagating states} \end{cases} \quad (50)$$

where $|\Delta_m| = \min\{|\Delta_1|, |\Delta_N|\}$ and $|\Delta_M| = \max\{|\Delta_1|, |\Delta_N|\}$. Criteria (47) and (50) differ strongly in a qualitative manner. First, the true criteria (47) are characterized by both Δ_1 and Δ_N because t_m and t_M are functions of both Δ_1 and Δ_N (see equations (48) and (49)). Second, the true criteria (47) depend on N explicitly, i.e., exhibit a size dependence. The importance of the size dependence will be made clearer later when investigating surface states in the next section. Yet, we note here that there is a study [22] which dealt with a similar problem for the particular case where $\Delta_1 = \Delta_N = \Delta \neq 0$. This work found the intuitive criteria (50) and was unable to predict the size dependence. As a consequence, the possibility of the existence of $N - 1$ propagating states was lost because for $\Delta_1 = \Delta_N$ (or equivalently $\Delta_m = \Delta_M$) the second line in (50) would disappear, and therefore only N or $N - 2$ propagating states would be possible. Our criteria (47) predict the existence of $N - 1$ propagating states even for $\Delta_1 = \Delta_N = \Delta$, since in this case t_m and t_M remain unequal: $t_m = (N - 1)|\Delta|/(N + 1)$, $t_M = |\Delta|$ and $t_M - t_m = 2|\Delta|/(N + 1)$. The N -dependence is of paramount significance for thin structures like OQWs which consist of just a few crystalline layers. For thick samples, when $N \gg 1$, the true and the intuitive criteria coincide practically because $\lim_{N \rightarrow \infty} t_{m,M} = |\Delta_{m,M}|$.

To complete this section, we find the coefficients α and β in equation (33) with the aid of equation (38) and the normalization condition for the wave function

$$1 = \langle \Psi | \Psi \rangle = \sum_{n=1}^N |g_n|^2. \quad (51)$$

As the result, we have obtained

$$\alpha = A\beta \quad A = -\frac{\Delta_1 \sin p}{\Delta_1 \cos p + R} \quad (52)$$

$$\beta^{-2} = \frac{N}{2}(A^2 + 1) + \frac{\sin Np}{2 \sin p} [(A^2 - 1) \cos(N + 1)p + 2A \sin(N + 1)p]. \quad (53)$$

5. Surface states

As is known, surface states can appear in structures which have surfaces, i.e., in finite or at least semi-infinite systems. The possibility of surface states dated back to Tamm's paper [23] and was studied in a good deal of work [24] quite a long time ago. All of the above-cited work considered a hypothetical model of a surface crystal which is obtained by cleaving between two adjacent planes and switching off all of the interactions between these two planes. Such a model, in fact, describes a semi-infinite system with a single surface and, thus, at most only one surface state may arise in the NLA. The OQW structure that we are considering here is of mesoscopic size and has two apparent surfaces.

The missing states in table 1 for case (i) are those resulting from case (ii) because these are the only two possible cases. Likewise, the true criteria (47) and the intuitive criteria (50) also imply, respectively,

$$\begin{cases} t_M \leq |R|: & \text{no surface states} \\ t_m \leq |R| < t_M: & \text{one surface state} \\ |R| < t_m: & \text{two surface states} \end{cases} \quad (54)$$

and

$$\begin{cases} |\Delta_M| \leq |R|: & \text{no surface states} \\ |\Delta_m| \leq |R| < |\Delta_M|: & \text{one surface state} \\ |R| < |\Delta_m|: & \text{two surface states.} \end{cases} \quad (55)$$

We shall examine criteria (54) for surface states emphasizing the importance of the size dependence. This requires a detailed analysis which will be carried out in what follows. For case (ii), instead of equation (33), we must resort to equation (35) to determine θ , ϑ , κ and j self-consistently. The two special equations (26) and (28) are satisfied if the parameters involved fulfil the following equations, respectively:

$$\theta [\Delta_1 e^\kappa + (-1)^j R] + \vartheta [\Delta_1 e^{-\kappa} + (-1)^j R] = 0 \quad (56)$$

$$\theta e^{N\kappa} [\Delta_N + (-1)^j R e^\kappa] + \vartheta e^{-N\kappa} [\Delta_N + (-1)^j R e^{-\kappa}] = 0. \quad (57)$$

Eliminating θ , ϑ from the above equations and introducing for brevity the notation $y = \exp \kappa$, we get

$$y^{2N} = \frac{\Delta_1 \Delta_N y^2 + (-1)^j R (\Delta_1 + \Delta_N) y + R^2}{R^2 y^2 + (-1)^j R (\Delta_1 + \Delta_N) y + \Delta_1 \Delta_N}. \quad (58)$$

Equation (58) will be solved graphically to determine the allowed values of the pairs (κ, j) . Among the various theoretical possibilities for the occurrence of surface states we shall consider two relevant cases. The first case corresponds to $\Delta_m \Delta_M < 0$ and $|\Delta_m| < |R| < |\Delta_M|$. In figure 3 we show both sides of equation (58) as a function of $y = \exp \kappa$ with the parameters $|R/\Delta_m| = 1.2$ and $|R/\Delta_M| = 0.85$. There is no solution for $N = 5$ and one solution for $N = 10$ (the trivial intersection at $y = 1$ is irrelevant). In general, there exists a critical number N^* determined by $|R/\Delta_m|$ and $|R/\Delta_M|$ through equations (54), (48) and (49) such that the number of surface states differs for $N \leq N^*$ and $N > N^*$. In the case under study we have one surface state for $N > N^*$ and no surface state for $N \leq N^*$. Here, for $|R/\Delta_m| = 1.2$ and $|R/\Delta_M| = 0.85$, we found N^* to be about 6. In the second case $\Delta_m \Delta_M > 0$ and $|R| < |\Delta_m| < |\Delta_M|$. If we choose $|R/\Delta_m| = 0.8$ and $|R/\Delta_M| = 0.5$, the critical number N^* is about 6. This is why we have two surface states for $N = 10$ ($> N^*$) and one surface state for $N = 5$ ($< N^*$) as seen from figure 4 and its inset. The above two numerical illustrations show the sensitivity of the number of surface states to the size of the OQW. This is because our theory reveals that the surface

state number is governed by t_m and t_M which depend not only on Δ_m and Δ_M but also on N . The energy location, is, however, ruled by the signs of Δ_m and Δ_M . A thorough sign analysis has led to the following sign rules. (i) If $\Delta_m \Delta_M > 0$ the surface state(s) is/are (it does not matter whether there is one or two of them) pushed up above (pulled down below) the band for $\Delta_M < 0$ ($\Delta_M > 0$). (ii) If $\Delta_m \Delta_M < 0$ and there is only one surface state, this state lies above (below) the band for $\Delta_M < 0$ ($\Delta_M > 0$). (iii) Nevertheless, if $\Delta_m \Delta_M < 0$ and there exist two surface states, they are always one above and one below the band.

Having solved for the allowed values of (κ, j) , we are now in the position to determine the coefficients θ and ϑ in equation (35). Either of equations (56) or (57), and the normalization condition, equation (51), are to be invoked for this purpose. We make use of equations (56) and (51) and arrive at the desired results:

$$\vartheta = \theta B \quad B = -\frac{\Delta_1 e^\kappa + (-1)^j R}{\Delta_1 e^{-\kappa} + (-1)^j R} \quad (59)$$

$$\theta^{-2} = C_N(\kappa) + 2B + B^2 C_N(-\kappa) \quad C_N(\kappa) = \frac{1 - e^{2N\kappa}}{e^{-2\kappa} - 1}. \quad (60)$$

6. Discussion

We have shown that in an N -layer OQW there are N eigenstates which can be classified into two kinds: propagating states and surface states. The number of surface states depends not only on the material parameters but also on the thickness. The latter dependence is manifested through the fact that within the NLA, for some parameter region, the number of surface states changes from $0 \rightarrow 1$ or $1 \rightarrow 2$ ($2 \rightarrow 1$ or $1 \rightarrow 0$) when the thickness increases (decreases). It is noticed that the maximal number of surface states is 2. This is because we have used the NLA. If one goes beyond the NLA—say, to the second-nearest-neighbour approximation—one has to handle more parameters: $E_1, E_2, E, E_{N-1}, E_N, R$ and R' where $E = E_n$ with $2 < n < N - 1$, $R = R_{n,n\pm 1}$ and $R' = R_{n,n\pm 2}$. Then, instead of three difference equations as in the NLA, there arise five equations which would give at most four surface states. The concept of ‘number of surface states’ is thus quite delicate. From a theoretical viewpoint, this concept is meaningful when a certain approximation for the interlayer coupling has been invoked. As mentioned in section 2, $R_{nn'}$ decreases quickly (in fact exponentially) with increasing $|n - n'|$ and the NLA proves to be a good approximation which has been widely used in the literature. From an experimental viewpoint, surface states respond to light in their own manner. Their number could be found from measurements of optical responses, which would suggest the theoretical approximation most suitable for the material structure under measurement.

Our theory is valid for any Δ_m and Δ_M . In particular, when $\Delta_m = \Delta_M = 0$ (the image effect is ignored), it follows from equations (48) and (49) that $|R| > t_m = t_M = 0$ always holds, yielding no surface states. We recover the result of [25], i.e., only solutions of propagating nature, $g_n = \sqrt{2/(N+1)} \sin(n\pi/(N+1))$, are possible. This very simple model for OQWs, whose boundary conditions are imposed by the so-called ‘no-escape requirement’, has been used by many authors just because of the simple analytic expression of its wave functions. A realistic model should account for the boundary conditions more carefully—at least as in the present paper. The semi-infinite surface crystal model is also obtained when one of Δ_m and Δ_M vanishes (the remaining parameter is denoted by Δ), and $N \rightarrow \infty$. In this limiting case, our theory gives $t_m = 0$, $t_M = |\Delta|$. Since $t_m = 0$, the condition $|R| < t_m = 0$ can never be fulfilled and the existence of two surface states is

impossible. Directly from equation (58) we now get

$$\lim_{N \rightarrow \infty} y^{2N} = \tilde{f}(y) \quad (61)$$

with

$$\tilde{f}(y) = -\frac{y - \tilde{y}}{\tilde{y}y(y - 1/\tilde{y})} \quad (62)$$

$$\tilde{y} = -\frac{(-1)^j R}{\Delta} \equiv -(-1)^j s_R s_\Delta \left| \frac{R}{\Delta} \right|. \quad (63)$$

The existence and location of the surface state is determined by the value and sign of \tilde{y} . For $(-1)^j R = \pm 1$ and $s_\Delta = \pm 1$ (or ∓ 1), we have $\tilde{y} = -|R/\Delta|$ (or $+|R/\Delta|$). Making use of the behaviour of the function $\tilde{f}(y)$, it is easy to verify that the condition for the surface state to exist and (a) to lie above the band is

$$\Delta \pm R < 0 \text{ and } \Delta < 0, \text{ or equivalently, } |\Delta| > |R| \text{ and } \Delta < 0 \quad (64)$$

and (b) to lie below the band is

$$\Delta \pm R > 0 \text{ and } \Delta > 0, \text{ or equivalently, } |\Delta| > |R| \text{ and } \Delta > 0. \quad (65)$$

These criteria are simply those reported for semi-infinite systems [24]. As a common result, we can conclude that the necessary conditions for two (one) surface states to appear are that both $\Delta_m \neq 0$ and $\Delta_M \neq 0$ simultaneously (either of Δ_m and Δ_M must differ from zero). In general, the absolute values of both of the ratios $|R/\Delta_m|$ and $|R/\Delta_M|$ determine the number of surface states (see criteria (47) and equations (48), (49)), while the signs of Δ_m and Δ_M place the energy levels of these states. The sign rules established in the text seem to be quite useful. According to these rules, if one knows the signs of Δ_m and Δ_M and the number of surface states, one is always able to definitely point out whether the surface state levels are located below or above the band. From an experimental point of view, one may turn this around and ask: if the number and the location of the surface states are known experimentally, may one provide information about the signs of Δ_m and Δ_M ? The answer is yes but not always definitely. When there are two surface states, the answer is definite. Namely, if both levels lie below (above) the band, this means that both Δ_m and Δ_M are positive (negative). Alternatively, if the two levels are one above and one below the band, this means that Δ_m and Δ_M have opposite signs. Nevertheless, when only one surface state arises, one cannot reach any definite conclusion regarding the signs of Δ_m and Δ_M .

It is also of interest to clarify the role that the sign of R plays. With this aim, let us return to any formulae associated with the surface state problem (see equations (36), and (56) to (58)). We become aware that R never stands alone but always enters with a factor $(-1)^j$ to form a combined quantity $(-1)^j R \equiv (-1)^j s_R |R|$. This combination is important since it determines the location of the surface state (see equation (36)). For a certain sign of R , j is 'selected' in such a way that $(-1)^j s_R$ together with κ must be solutions of equation (58). Thus, the sign of R does not play any role in forming surface states ($\text{sign}(R)$ is, however, important in problems concerning the optical responses).

Attention is now to be paid to the image effect in more detail. Theoretically, the parameters Δ_m and Δ_M can be evaluated using the formulae in section 2. Let us for simplicity suppose that the molecules have inversion symmetry. Then in the dipole approximation the A - and \tilde{A} -terms vanish. We have evaluated the remaining dipole sums by Fourier transforming them into sums over the corresponding reciprocal-lattice vectors

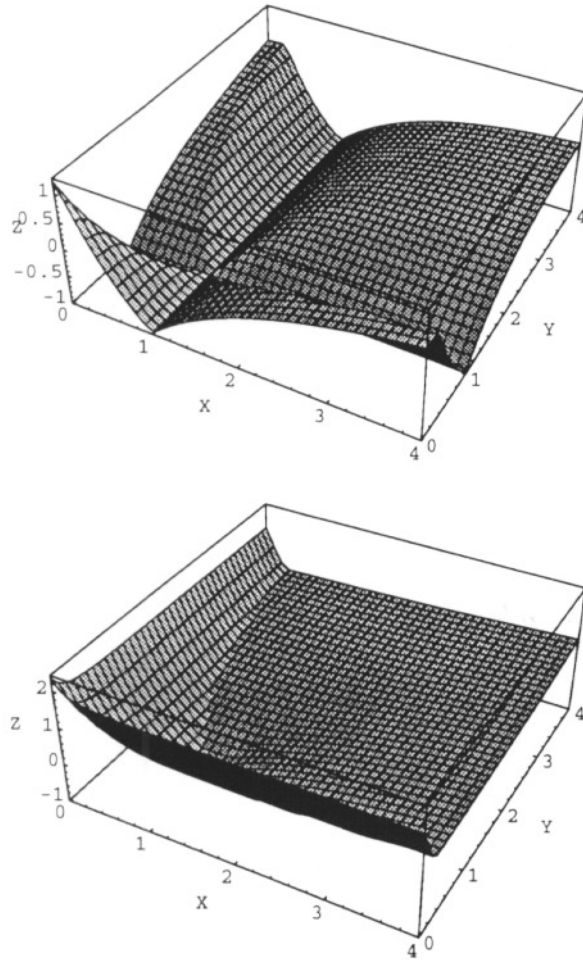


Figure 5. $Z = t_m/|R| - 1$ (upper panel) and $Z = t_M/|R| - 1$ (lower panel) versus $X = \varepsilon_1/\varepsilon$ and $Y = \varepsilon_2/\varepsilon$ for $\gamma_1 = \gamma_2 = 0.9$ and $N = 5$.

[17, 18]. As a result, we obtain for $\boldsymbol{\mu} \parallel (\mathbf{a}, \mathbf{b})$ plane ($\boldsymbol{\mu}$ is the dipole moment of a molecule which is assumed to be the same for all molecules)

$$\Delta_1^{\parallel} = -\frac{\varepsilon - \varepsilon_1}{\varepsilon(\varepsilon + \varepsilon_1)} W(\gamma_1) \quad (66)$$

$$\Delta_N^{\parallel} = -\frac{\varepsilon - \varepsilon_2}{\varepsilon(\varepsilon + \varepsilon_2)} W(\gamma_2) \quad (67)$$

$$R^{\parallel} = \frac{1}{\varepsilon} W(1) \quad (68)$$

where $\gamma_{1,2} = 2d_{1,2}/c$ and $W(z)$ is (\mathbf{g} is a two-dimensional reciprocal-lattice vector)

$$W(z) = \frac{2\pi^2\mu^2}{ab} \sum_{\mathbf{g}} |\mathbf{g} + \mathbf{k}| e^{-2\pi z c |\mathbf{g} + \mathbf{k}|}. \quad (69)$$

For $\boldsymbol{\mu} \perp (\mathbf{a}, \mathbf{b})$ plane, we get $\Delta_{1,N}^{\perp} = 2\Delta_{1,N}^{\parallel}$ and $R^{\perp} = -2R^{\parallel}$. The image effect caused by

the abrupt change in the dielectric constants is clearly seen from the above equations. Here the parameters d_1 and d_2 exhibit their role. For $2d_1 = 2d_2 = c$, i.e., $\gamma_1 = \gamma_2 = 1$, we get for both of the orientations of μ the following simple ratios:

$$\left| \frac{\Delta_1}{R} \right| = \left| \frac{1 - \varepsilon_1/\varepsilon}{1 + \varepsilon_1/\varepsilon} \right| \quad \left| \frac{\Delta_N}{R} \right| = \left| \frac{1 - \varepsilon_2/\varepsilon}{1 + \varepsilon_2/\varepsilon} \right|. \quad (70)$$

These formulae indicate that $|R|$ is greater than $|\Delta_M| = \max\{|\Delta_1|, |\Delta_N|\}$ for any ε , ε_1 and ε_2 (the same result is obtained for $2d_1, 2d_2 > c$). Hence, for surface states to exist, it is necessary to have $0 < d_1, d_2 < c/2$ (i.e., $0 < \gamma_1, \gamma_2 < 1$). Figure 5 shows $t_m/|R| - 1$ and $t_M/|R| - 1$ as functions of $\varepsilon_1/\varepsilon$ and $\varepsilon_2/\varepsilon$ for $\gamma_1 = \gamma_2 = 0.9$ obtained using the following parameters: $k = 0$, $a = 12 \text{ \AA}$, $b = 6 \text{ \AA}$, $c = 23 \text{ \AA}$ (close to the lattice constants of orthorhombic $\text{C}_{14}\text{H}_{10}\text{CuO}_4^*$) and $N = 5$. It is apparent from figure 5 that, for $\gamma_1 = \gamma_2 = 0.9 (< 1)$, there are domains of $\varepsilon_1/\varepsilon$ and $\varepsilon_2/\varepsilon$ in which one ($t_m/|R| - 1 < 0 < t_M/|R| - 1$) or two ($0 < t_m/|R| - 1 < t_M/|R| - 1$) surface states may arise. For a given OQW material, ε_1 , ε_2 , d_1 and d_2 serve as control parameters for tailoring the electronic energy spectrum of the OQW. For example, as is often encountered in experiments, one can choose $\varepsilon_2 \approx 1$ (air). Then, from equation (67) one gets $\Delta_N < 0$ because ε is always greater than 1. The sign of Δ_1 can be made positive or negative by choosing $\varepsilon_1 > \varepsilon$ or $\varepsilon_1 < \varepsilon$, correspondingly (see equation (66)). If one knows the interface distances d_1 and d_2 , one can calculate the energy spectrum of the OQW. In contrast, if d_1 and d_2 are unknown, experimental data from the OQW energy spectrum would provide information about the magnitudes of the interface distances.

Optical responses of surface organics have been studied experimentally mainly for anthracene [26, 27]. In crystals like anthracene, tetracene, . . . , the energy difference between the internal and surface layers ($\sim -200 \text{ cm}^{-1}$) is much greater than the interlayer interaction ($\sim 1 \text{ cm}^{-1}$). Under such circumstances, the electronic structure can be approximately regarded as being composed of excitations from the isolated top surface layer, the one immediately below, etc. For anthracene, the exciton energy level of the top surface layer is found at 204 cm^{-1} above the bulk A-exciton one, and that of the layer below is also weakly observed at only 6 cm^{-1} above the bulk one. A very sharp dip structure was observed in the reflection spectrum, and was attributed to the exciton of the top surface layer [28]. Picosecond time-scale measurements [26] at low temperatures have shown super-radiant decays of about or shorter than 2 ps for the top-surface-layer exciton and of the order of 15 ± 2 ps for the exciton from the layer below. However, in fact, the interlayer interaction R , though it may be very small in comparison with Δ_1 and Δ_N , never equals zero exactly. The $R \neq 0$ correction to the optical responses may be small for anthracene, tetracene, . . . , but may not be negligible for other organics in general. In order to obtain a deeper understanding of the optical responses of anthracene, tetracene, . . . and to anticipate new optical properties of other organics, in which the interlayer interaction is not too small compared with other energy characteristics, we must extend the present theory in a few directions. First, we should couple the OQW to the radiation field and calculate the imaginary part of the exciton self-energy due to this coupling, on the basis of the electronic structures of multilayer OQWs obtained in the way described in this paper. Original surface states due to $R \neq 0$ should be taken into account instead of those of noninteracting layers. Second, if necessary, our theory can be extended beyond the NLA, i.e., to take into account the coupling with the second, third, . . . nearest layers. The number of possible surface states will increase and the theoretical formulation will be much more complicated. Third, the unit cell was assumed to contain a single molecule, so the effect of Davydov splitting cannot be discussed within the present theory. The extension necessary to take account of

this effect is straightforward but worth doing. The transition dipole moment in the (\mathbf{a}, \mathbf{b}) plane of anthracene is so large that the exciton energy dispersion in the \mathbf{k} direction ($\parallel (\mathbf{a}, \mathbf{b})$ plane) becomes of the order of 500 cm^{-1} above that of the bulk A exciton at $k = 0$. On the other hand, in the \mathbf{p} direction ($\perp (\mathbf{a}, \mathbf{b})$ plane), the exciton energy dispersion may be smaller because of the interlayer distance being larger than the lattice constants in the (\mathbf{a}, \mathbf{b}) plane. The surface state is above the band in the \mathbf{p} direction, but is embedded within the width of the energy band in the \mathbf{k} direction. The mixing of the surface states with the bulk states looks very slight at low temperatures. However, the above features would change drastically in organics in which the interlayer separation is of the same order as or smaller than the lattice constants in the layer planes, leading to strong coupling between layers. Fourth, it is also an interesting future problem to explain the various dynamical characteristics of surface states in thick as well as thin OQWs by simultaneously taking into account the interactions with both the photon field and the phonon field on the basis of the correct electronic structures. Last but not least, the problems of surface quality (roughness, random distribution of molecules on surfaces, surface relaxation and polarization, ...) are quite delicate.

Acknowledgments

The authors are indebted to Professor V M Agranovich for providing them with an article [9] prior to publication, and to Professors K Miyano, M Kuwata-Gonokami, K Cho, H Ueba, H Ishihara, Y Ohfuti, M Yamanishi, T Ishihara and M Ueda for fruitful discussions. Part of this work was supported by JSPS and by a Grant-in-Aid for Scientific Research on the Priority Area 'Mutual and Quantum Control of Radiation and Electronic Systems' from the Ministry of Education, Science and Culture of Japan. Funds from SAREC to finance the current Associateship visit of one of us (NBA) at ICTP are gratefully acknowledged. NBA would also like to thank the ICTP's Condensed Matter Physics Group for hospitality.

References

- [1] See, e.g.,
Weisbuch C and Vinter B 1991 *Quantum Semiconductor Heterostructures* (Boston, MA: Academic)
- [2] See, e.g.,
Zyss J 1994 *Molecular Nonlinear Optics* (Boston, MA: Academic)
- [3] So F F, Forrest S R, Shi Y Q and Steier W H 1990 *Appl. Phys. Lett.* **56** 674
Zang D Y, Shi Y Q, So F F, Forrest S R and Steier W H 1991 *Appl. Phys. Lett.* **58** 562
So F F and Forrest S R 1991 *Phys. Rev. Lett.* **66** 2649
- [4] Hoshi H, Kohama K, Fang S and Maruyama Y 1993 *Appl. Phys. Lett.* **62** 3080
- [5] Agranovich V M and Zakhidov A A 1979 *Chem. Phys. Lett.* **68** 86
Agranovich V M, Atanasov R D and Bassani G F 1992 *Chem. Phys. Lett.* **199** 621
Agranovich V M 1993 *Mod. Cryst. Liq. Cryst.* **230** 13
Agranovich V M and Dubovsky O A 1993 *Chem. Phys. Lett.* **210** 458
Agranovich V M and Ilinski K N 1994 *Phys. Lett.* **191A** 309
Agranovich V M, Atanasov R A and Bassani G F 1994 *Solid State Commun.* **92** 295
- [6] Leegwater J A and Mukamel S 1992 *Phys. Rev. A* **46** 452
Wang N, Jenkins J K, Chernyak V and Mukamel S 1994 *Phys. Rev. B* **49** 17079
- [7] Ishihara H and Cho K 1992 *Int. Nonlinear Opt. Phys.* **1** 287; 1993 *Mod. Cryst. Liq. Cryst. Sci. Technol.* **B 4** 81
- [8] Munn R W 1993 *Mod. Cryst. Liq. Cryst.* **228** 23
- [9] Agranovich V M, Dubovsky O A, Grigorishin K I, Leskova T A and Reineker P 1996 to be submitted
- [10] Tokihiro T, Manabe Y and Hanamura E 1993 *Phys. Rev. B* **47** 2019; 1995 *Phys. Rev. B* **51** 7655
- [11] Schlosser D W and Philpott M R 1980 *Chem. Phys.* **49** 181

- [12] See, e.g.,
Silinsh E A 1980 *Organic Molecular Crystals* (Berlin: Springer)
- [13] Haskal E I, Shen Z, Burrows P E and Forret S R 1995 *Phys. Rev. B* **51** 4449
- [14] Kataoka T, Kondo T, Ito R, Sasaki S, Uchida K and Miura S 1993 *Phys. Rev. B* **47** 2010
- [15] Muljarov E A, Tikhodeev S G, Gippius N A and Ishihara T 1995 *Phys. Rev. B* **51** 14370
- [16] Agranovich V M 1993 *Mol. Cryst. Liq. Cryst.* **230** 13
- [17] Nguyen Ba An and Hanamura E 1995 *Phys. Lett.* **199A** 249
- [18] Nijboer B R A and De Wette F W 1957 *Physica* **23** 309; 1957 *Physica* **24** 422
Philpott M R 1973 *J. Chem. Phys.* **58** 588
Bounds P J and Munn R W 1979 *Chem. Phys.* **44** 103; 1981 *Chem. Phys.* **59** 47
- [19] Agranovich V M and Galanin M D 1982 *Electronic Excitation Energy Transfer in Condensed Matter* ed V M Agranovich and A A Maradudin (Amsterdam: North-Holland)
- [20] Keldysh L V 1979 *Pis. Zh. Eksp. Teor. Fiz.* **29** 716
Hanamura E, Nagaosa N, Kumagai M and Takagahara T 1988 *Mater. Sci. Eng. B* **1** 255
Kumagai M and Takagahara T 1989 *Phys. Rev. B* **40** 12359
Tran Thoai D B, Zimmermann R, Grundmann M and Bimberg D 1990 *Phys. Rev. B* **42** 5906
Betbeder-Matibet O and Combescot M 1995 *Solid State Commun.* **94** 221
- [21] Koster G F and Slater J C 1954 *Phys. Rev.* **95** 1167
- [22] Sugakov V I 1964 *Sov. Phys.–Solid State* **5** 1607; 1973 *Sov. Phys.–Solid State* **14** 1711
- [23] Tamm I 1932 *Phys. Z. Sowjetunion* **1** 733
- [24] Pekar S I 1958 *Sov. Phys.–JETP* **6** 785
Agranovich V M, Mal'shukov A G and Mekhtiev M A 1972 *Sov. Phys.–Solid State* **14** 725
Stern P S and Green M E 1973 *J. Chem. Phys.* **58** 2507
Hoshen J and Kopelman R 1974 *J. Chem. Phys.* **61** 330
Schipper P E 1975 *Mol. Phys.* **29** 501
Philpott M R and Turllet J M 1976 *J. Chem. Phys.* **64** 3852
Ueba H and Ichimura S 1976 *J. Phys. Soc. Japan* **41** 1974; 1977 *J. Phys. Soc. Japan* **42** 355
Ueba H 1977 *J. Phys. Soc. Japan* **43** 353
Ueba H and Ichimura S 1979 *J. Chem. Phys.* **70** 1745
- [25] Mahan G D and Obermair G 1969 *Phys. Rev.* **183** 182
- [26] Aaviksoo Ya, Lippamaa Ya and Reinot T 1987 *Opt. Spectrosc.* **62** 706
- [27] Kuwata-Gonokami M 1995 private communications
- [28] See, e.g.,
Turllet J M, Kottis P and Philpott M R 1983 *Advances in Chemical Physics* vol 54 (New York: Wiley)